# Unusual binding of Grb2 protein to a bivalent polyproline-ligand immobilized on a SPR sensor: Intermolecular bivalent binding

Nico de Mol, John A. W. Kruijtzer, Ed Moret, Isabelle Broutin, Rob M. J. Liskamp

# Unusual binding of Grb2 protein to a bivalent polyproline-ligand immobilized on a SPR sensor: Intermolecular bivalent binding

Nico de Mol, John A.W. Kruijtzer, Ed Moret, Isabelle Broutin, Rob M.J. Liskamp

# Unusual binding of Grb2 protein to a bivalent polyproline-ligand immobilized on a SPR sensor: Intermolecular bivalent binding

Nico J. de Mol [a,*], John A.W. Kruijtzer [a], Ed E. Moret [a], Isabelle Broutin [b], Rob M.J. Liskamp [a]

[a] Department of Medicinal Chemistry & Chemical Biology, Utrecht Institute of Pharmaceutical Sciences, Universiteitsweg 99, 3484 CG Utrecht, The Netherlands
[b] Laboratoire de Cristallographie et RMN Biologiques, Faculté de Pharmacie, Université René Descartes, 4 Avenue de l'Observatoire, 75270 Paris Cedex 06, France

ARTICLE INFO

*Article history:*
Received 23 March 2012
Received in revised form 22 October 2012
Accepted 5 November 2012
Available online 15 November 2012

*Keywords:*
Grb2
Polyproline
SH3-domain
Sos-protein
Surface plasmon resonance (SPR)
Divalent binding

ABSTRACT

The Grb2 adapter protein is involved in the activation of the Ras signaling pathway. It recruits the Sos protein by binding of its two SH3 domains to Sos polyproline sequences. We observed that the binding of Grb2 to a bivalent ligand, containing two Sos-derived polyproline-sequences immobilized on a SPR sensor, shows unusual kinetic behavior. SPR-kinetic analysis and supporting data from other techniques show major contributions of an *inter*molecular bivalent binding mode. Each of the two Grb2 SH3 domains binds to one polyproline-sequence of two *different* ligand molecules, facilitating binding of a second Grb2 molecule to the two remaining free polyproline binding sites. A molecular model based on the X-ray structure of the Grb2 dimer shows that Grb2 is flexible enough to allow this binding mode. The results fit with a role of Grb2 in protein aggregation, achieving specificity by multivalent interactions, despite the relatively low affinity of single SH3 interactions.

## 1. Introduction

The Grb2 protein is an adapter protein linking activation of receptor tyrosine kinases (RTKs), cytokine- and antigen-receptors, to the Ras signaling pathway (Fig. 1A). Examples of such receptors are growth factor receptors, the insulin receptor, and the T-cell receptor. The Ras protein controls major signaling routes of cell proliferation, differentiation and survival; its deregulation plays a critical role in the development of tumors [1].

The Grb2 protein consists of a central SH2 domain, to which two SH3 domains are connected by flexible linkers (Fig. 1B). The SH2 domain is involved in recruiting Grb2 to the RTKs directly, or indirectly through the adaptor proteins Shc and LAT (Fig. 1A), by binding to phosphotyrosines (pY's) in a specific sequence. The SH3 domains bind to proline-rich sequences adopting a type II polyproline (PPII) helix [2]. Grb2 binds to polyproline (PP) sequences of the guanylnucleotide exchange factor Sos. In this way upon RTK-activation, Sos protein is recruited to the plasma membrane, where it is able to activate membrane-bound Ras by GDP/GTP exchange. The C-terminal region of Sos contains at least four PP-sequences that are recognized by the Grb2 SH3 domains [3]. In addition to the simple linear model shown in Fig. 1A, now also the involvement of other proteins is emerging, like Gab1, which also binds with its PP-sequences to Grb2 [1,4].

The crucial role of the Grb2-Sos interaction in the activation of the Ras pathway suggests that high affinity molecules interfering in Grb2-protein complexes are useful in a therapeutic strategy for tumors, and particularly certain types of leukemia [5–7]. Exploring the expected higher affinity of a bivalent interaction, Cussac et al. made a proline-rich peptide construct designed for bivalent binding to both Grb2 SH3 domains [8]. This construct was modified to enter cells and indeed was able to inhibit signaling events downstream from the Sos-Grb2 interaction [8]. Yuzawa et al. also designed peptides with two PP-sequences connected by linkers of varying length [9]. Also in this case bivalent binding was much stronger than monovalent binding.

Apart from the interest in intervention in SH3-protein interactions for therapeutic purposes, there is a more fundamental reason to address the question how relatively low affinity interactions of SH3 domains (typically around $10^{-5}$ M) can play a role in determining specificity of protein interaction networks [3,10]. Specificity is enhanced by multivalent interactions involving SH3 domains. Adapter proteins like Grb2 and Crk contain two SH3 domains, Nck even three. Although many details on the role of SH3-multiplicity on a molecular level still has to be uncovered, a picture is emerging that interactions with these SH3 domains play a central role in the formation of multi-component clusters of proteins [10].

*Abbreviations:* PP, polyproline; RTK, receptor tyrosine kinase; $K_{LM}$, apparent Langmuir binding constant; $K_S$, binding constant in solution derived from SPR competition experiments

* Corresponding author at: PO Box 80082, 3508 TB Utrecht, The Netherlands. Tel.: +31 6 20246115; fax: +31 30 253 6655.
*E-mail address:* N.J.deMol@uu.nl (N.J. de Mol).

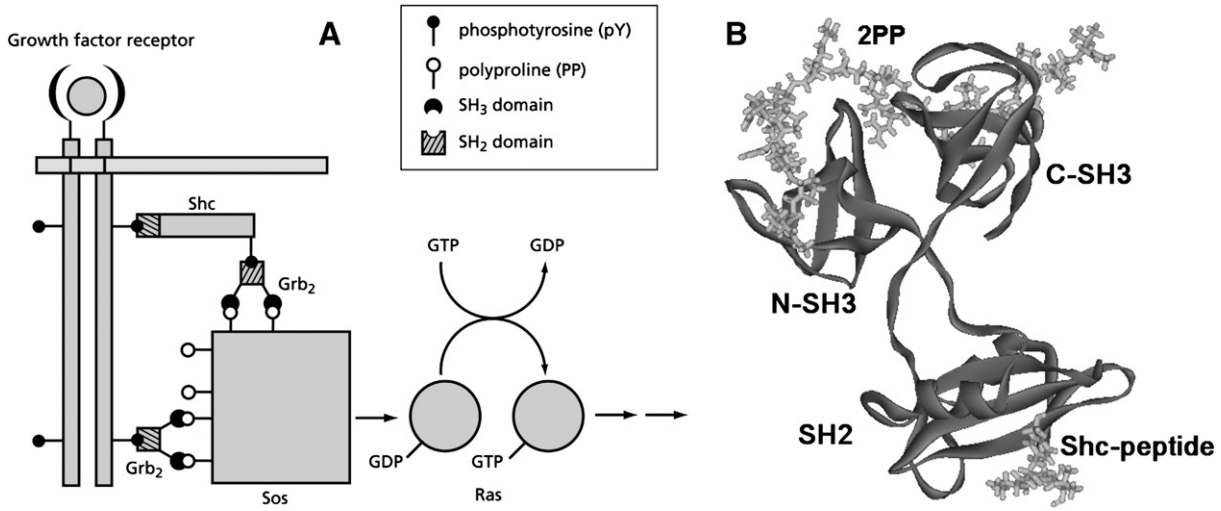


**Fig. 1.** (A) Simplified scheme depicting the role of Grb2 in direct Ras activation, Grb2 binds through its SH2 domain to a receptor tyrosine kinase (RTK) and through its SH3 domains it recruits the nucleotide exchange factor Sos, which operates on the Ras protein. (B) Grb2 in the X-ray conformation (PDB ID: 1GRI, ribbons), modeled in complex with a bivalent polyproline ligand, as used in this study (**2PP**, see Section 2.8), *intra*molecularly bivalently bound to both SH3 domains. The SH2 domain is shown in complex with a phosphotyrosine (pY) containing peptide (pYVNV) derived from the Shc protein. Peptides are represented as sticks.

Attempting to study the binding of Grb2 with proline-rich sequences more in detail, we started a study of the kinetics of this interaction using SPR. Because of the reported high affinity of the proline-rich peptidodimer of Cussac et al. [8], we synthesized this ligand (referred to as **2PP**). The two PP-epitopes in **2PP** are identical and derived from a PP sequence in Sos. Kinetic measurements were performed using SPR, with **2PP** immobilized on an SPR surface. Such surfaces mimic the multiple PP sequences on protein surfaces. For example, the C-terminus of the Sos protein contains seven PP-sequences, which meet the consensus sequence for class I or class II [2]. At least four of these have been shown to bind to Grb2 SH3 domains [3].

It was found that the kinetics of binding of Grb2 to the 2PP-surface was deviant from other bivalent binding systems: the appearance of the association and dissociation phase was clearly biphasic. The observed kinetics is consistent with a binding model in which bivalent binding is not as expected *intra*molecular (one **2PP** binds bivalent to one Grb2 molecule, as shown in Fig. 1B), but rather *inter*molecular: both SH3 domains of one Grb2 molecule bind each one PP-epitope from two *different* immobilized **2PP** molecules. The remaining two empty PP-epitopes generate a binding site for a second Grb2 molecule (see Scheme 1).

## 2. Materials and methods

### 2.1. Peptide synthesis

The peptides **1PP** and **2PP** (Fig. 2), based on the VPPPVPPRRR (hSos1 1149–1158) sequence, were assembled on an automatic ABI 433A Peptide Synthesizer using the ABI FastMoc 0.25 mmol protocols (*Applied Biosystems Model 433A Peptide Synthesizer User's Manual* June 1993, Version 1.0; *Applied Biosystems Research News* June 1993, Model 433A Peptide Synthesizer, 1–12), except that the coupling time was 45 min instead of 20 min. Fmoc (9-fluorenylmethoxycarbonyl)-amino acid derivatives, activated in situ using HBTU/HOBt and DiPEA in NMP, were used in coupling steps.

**2PP** was synthesized by incorporating Fmoc-Lys(Fmoc)-OH at the appropriate position in the peptide and after removal of the Fmoc-groups the two remaining peptide sequences were coupled simultaneously to both the ε- and α-amino groups of the lysine.

The peptides were deprotected and cleaved from the resin by treatment with 25 mL TFA/$H_2O$/TIS (95:2.5:2.5), for 2 h at room temperature. Finally, the peptides were precipitated in a MTBE/n-hexane (1/1, v/v) solution.

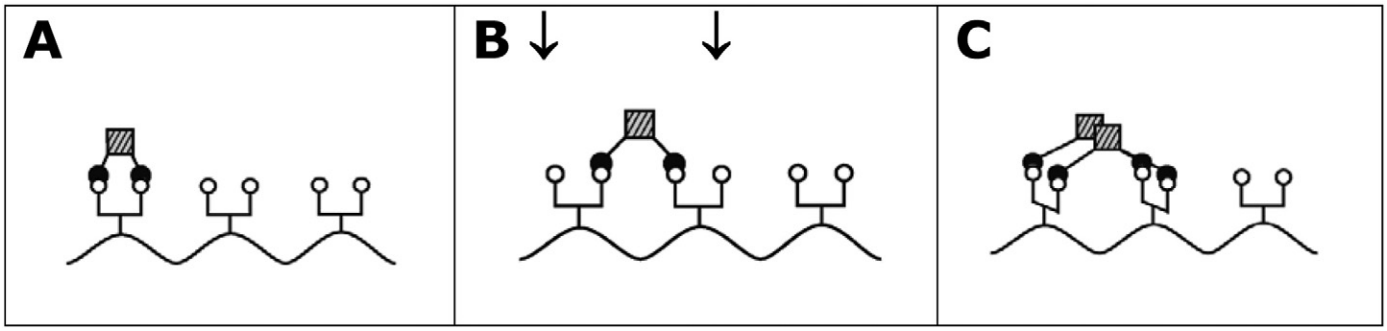


**Scheme 1.** Schematic representation of species involved in bivalent binding of a bivalent analyte (full circles) to an immobilized bivalent ligand (open circles). A: *intra*molecular bivalent binding, see also the model in Fig. 1B. B: *inter*molecular bivalent binding. C: *inter*molecular bivalent binding with binding of a second analyte molecule on the remaining empty binding sites indicated by arrows in panel B.

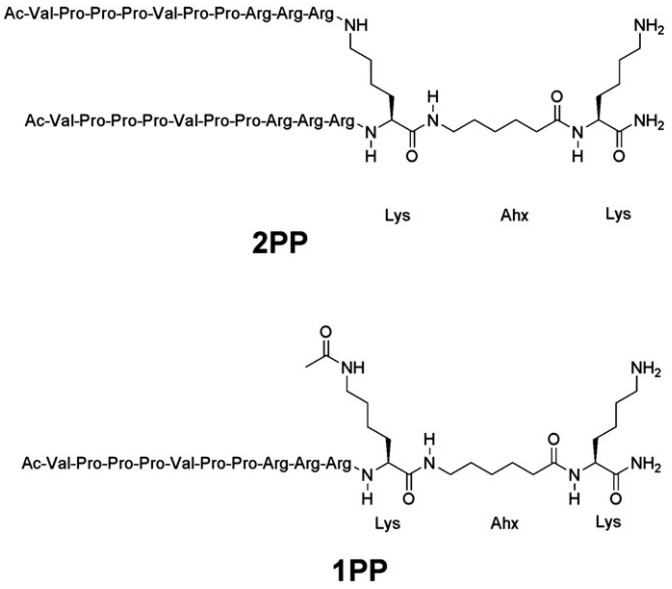


**Fig. 2.** Synthesized monovalent (**1PP**) and bivalent (**2PP**) polyproline peptide based on the hSos1 sequence (1149–1158). Here the peptides are shown including a 6-aminohexanoic acid-lysine (Ahx-Lys) linker for immobilization on the SPR sensor. For competitive assays and dissociation experiments **1PP** and **2PP** were used without this extension, and with an amide on the Lys carboxyl group.

After this, the pellets were dissolved in *tert.*-BuOH/water (1/1, v/v) (ca. 60 mL) and lyophilized to obtain the crude peptides as white fluffy solids. The peptides **1PP** and **2PP** were purified by preparative HPLC on a Phenomenex Jupiter C4 (300 Å, 10 μm, 250 × 21.2 mm) column and a linear gradient from 100% A (0.1% TFA in water/acetonitrile (95/5)) to 35% B (0.1% TFA in water/acetonitrile (60/40)) over 60 min at a flow rate of 12 mL/min, with detection at 214 nm.

The peptides were characterized by analytical HPLC (**1PP**: 100% and **2PP**: 96%) and by MALDI-TOF (**1PP**: monoisotopic mass $[M+H]^+$ calcd for $C_{75}H_{132}N_{25}O_{15}$, 1623.0335; found, 1623.1050 and **2PP**: monoisotopic mass $[M+H]^+$ calcd for $C_{128}H_{221}N_{44}O_{25}$, 2774.7375; found, 2774.5190).

### 2.2. Grb2 protein expression and purification

Full length Grb2 protein was expressed and purified as described [11]. In short, the protein was expressed as a GST-fused protein and purified by affinity chromatography on glutathione agarose beads. To increase the stability the two cysteines C32 and C198 were replaced by serines. Grb2 was eluted from the beads by cleavage of the GST moiety with thrombin. Part of the protein was obtained as a stable Grb2-dimer. Separated fractions of GST-free Grb2 dimer and monomer were obtained from a Mono Q ion exchange chromatography column. Experiments were performed with the monomeric form, except that the dimer was used as a positive control in chemical cross-linking experiments.

### 2.3. SPR binding experiments

SPR experiments were performed, both with a Biacore 3000 (GE Healthcare) and with a two-channel IBIS II instrument (Ecochemie, Utrecht, The Netherlands). The Biacore3000 was equipped with Biacore CM5 chips (GE Healthcare) and the IBISII with Xantec CMD6 sensor chips (Xantec, München, Germany). Both these chips are covered with a carboxymethyldextran thin layer in brush conformation on the gold surface, and have comparable properties. Coupling of **1PP** and **2PP**-peptides, elongated with an N-terminal 6-aminohexanoic acid-lysine (Ahx-Lys) spacer, was performed in 10 mM maleate buffer pH 7.0, through the Lys-ε-$NH_2$ group in the spacer, using standard EDC/NHS chemistry. The spacer in the peptides is introduced to avoid any sterical clashes between the bound Grb2 protein and the dextrin matrix of the sensor chip. Surfaces with different binding capacities were obtained by varying the concentration of the peptide and the reaction time. Of the four flow cells of the Biacore3000, nr 1 was used as a reference (only EDC/NHS activation and blocking with ethanolamine), in nr 2 and 3 **2PP** was coupled for a high and low binding capacity surface, by exposing the EDC/NHS activated surface with 0.1 mM elongated **2PP** during 1 min, and 2 μM **2PP** during 1 min, respectively. Flow cell 4 was immobilized with the elongated **1PP** peptide (1 mM during 20 min). After immobilization unreacted activated carboxyl groups were blocked with 1 M ethanolamine. For immobilization on the CMD6 chips in the IBISII for high density surfaces typically 2 mM **2PP** or **1PP** during 10 min was used. For medium and low binding capacity this was 0.5 mM peptide during 10 min, and 0.5 mM during 2 min, respectively. Again the reference cell was only activated with EDC/NHS and blocked.

Running buffer in all SPR binding experiments was Hepes buffer pH 7.4 (10 mM Hepes, 3.4 mM EDTA, 150 mM NaCl and 0.005% Tween-20). Between measurements the surface was regenerated with 0.2% SDS in 50 mM HCl. In the Biacore the flow-rate was generally 40 μL/min.

Binding isotherms based on the equilibrium signal from the SPR curves with different Grb2 concentrations were analyzed with the Langmuir equation:

$$R_{eq} = \frac{[Grb2]}{[Grb2] + K_{LM}} . B_{\max}. \quad (1)$$

This yields the apparent Langmuir binding constant $K_{LM}$ and the maximum binding capacity $B_{max}$.

The Biacore instrument measures the SPR signal in RU units, the IBIS II in millidegree (m°). 1 RU corresponds to 10 m°, for easier comparison of the SPR signals, in the presented data RU units have been converted into m°.

### 2.4. Kinetic analysis

Kinetic analysis was performed using the program CLAMP from Morton and Myzska [12]. In a global kinetic analysis using CLAMP, several experimental SPR curves, i.e. with various Grb2 concentrations, are analyzed simultaneously, using the same fit parameters. The experimental data are fitted to predefined binding models. The quality of the fit is indicated by the residual sum of the squared difference between the measured and simulated data (RSSq-value), by approximation the mean deviation per data point of the experimental value from the fitted value.

### 2.5. Displacement studies

Association of 1 μM Grb2 was either very short (10 s) or was allowed to reach equilibrium. Then manually 10 μL **1PP** was added in a concentration range ($10^{-6}$ to $10^{-3}$ M). In separate experiments the bulk effect of these peptide concentrations was assayed. The remaining percentage of the original binding without added peptide, corrected for any bulk effect, is determined.

### 2.6. Chemical cross-linking experiments

10 μL $2 \times 10^{-5}$ M Grb2 in HGNED buffer pH 8 was mixed with 8 μL $5 \times 10^{-4}$ M 2PP in HGNED buffer. HGNED buffer is 25 mM HEPES, 100 mM NaCl, 0.2 mM EDTA. 0.05% (v/v) NP-40, 10% glycerol and 1 mM DTT, added immediately before use. To this mixture 2 μL of glutaraldehyde with a concentration range from 0.1 to 10% was added. After 10 min 2 μL of quencher solution (1 M Tris and 1 M glycine, pH 7.5) was added. 10 μL of these samples was mixed with 10 μL of

SDS-PAGE buffer, and 2 μL samples was analyzed by SDS-PAGE using PhastGel homogeneous-20 gels (GE Healthcare) and Coomassie brilliant blue staining.

### 2.7. Dynamic light scattering experiments

The mean particle size distribution of protein solutions was analyzed by dynamic light scattering, using an ALV CGS-3 instrument (ALV, Langen, Germany) at 25 °C. First an 80 μM Grb2 solution in HBS, filtered through a 0.2 μm filter was measured. Then to 500 μL of this solution, 20 μL of filtered 5 mM **2PP** solution was added, resulting in a final concentration of approximately 200 μM. This solution was also measured. Based on the $K_D$ for Grb2 binding to **2PP**, as assayed in this study, under these conditions >99% of Grb2 is bound.

### 2.8. Modeling of bivalent 2PP — Grb2 complexes

The model with *intra*molecular bivalently bound **2PP** to Grb2 (Fig. 1B, Scheme 1A) was generated by superpositioning of the NMR structure of the N-SH3 domain in complex with Sos peptide Ac-VPPPVPPRRR-$NH_2$ (PDB ID: 1GBQ) on the N-SH3 domain in the X-ray Grb2 structure (PDB ID: 1GRI). The NMR structure was used to supply the missing coordinates for the residues 28–33 in the Grb2 structure, as well as to supply the Sos peptide. The Grb2 SH2 structure with the Shc derived pYVNV-peptide (PDB ID: 1JYR) was used to supply the Shc peptide. All superimpositions were made with the MOTIF program [13]. To obtain the Sos peptide in the C-SH3 domain, it was manually docked in class II orientation into this domain. The lysine linker between the two PP-peptides was attached to complete the **2PP** ligand, followed by minimization and simulated annealing, keeping the Grb2 protein in the X-ray structure.

The model with *inter*molecular bivalent binding of 2 Grb2 molecules to 2PP (Scheme 1C, Fig. 12) was generated by swapping of the N-SH3 domains in the X-ray dimer structure (PDB ID: 1GRI). The SH2-N-SH3 linker of molecule 1 was cut at position Glu54 near the N-SH3 domain and positioned in the direction of the N-SH3 domain of molecule 2, and fused to the proper position of this N-SH3. The same procedure was applied to the SH2-N-SH3 linker of molecule 2. The linker length was sufficient to allow the swapped structure. After this the linkers to all four SH3 domains (residues Glu54-Lys64 and Gln153-Gln162) were minimized with steepest descent and simulated annealing, keeping the rest of the dimer structure in fixed position. This allows relaxed SH2–SH3 linkers in the model. The **2PP** peptide was placed in a manner analogous to the *intra*molecular bivalent complex (see Fig. 12A). Modeling and simulated annealing simulations were performed *in vacuo* in Yasara Structure 7.11.28 [14]. The Amber99 force field with its default settings was used [15].

## 3. Results

### 3.1. Synthesized compounds

The PPII helix conformation of PP-ligands bound to SH3 domains is quite similar in overall structure when viewed from its N- or C-terminus. These ligands can bind in either of two orientations: class I or class II [10]. The C-terminus of the Sos protein contains seven proline-rich sequences that exactly meet the consensus sequence for these classes. Not all of these sequences have been screened for binding to Grb2 SH3 domains, but the four that have been, indeed bind to Grb2 SH3 [2]. Next to these, several other proline-rich sequences are present in the Sos C-terminus that do not exactly match the consensus sequence.

Cussac et al. reported a high affinity for Grb2 of a bivalent ligand based on the VPPPVPPRRR (hSos1 1149–1158) sequence [8]. Therefore a bivalent (**2PP**) and a monovalent (**1PP**) peptide were synthesized with this sequence incorporated (Fig. 2). The bivalent **2PP** is nearly identical to that made by Cussac et al., except that in our peptides the N-terminus of the PP-sequence is acetylated. Furthermore, to avoid steric crowding of Grb2 on the SPR sensor matrix, the peptides for coupling to the sensor chip were extended with an Ahx-Lys spacer (Fig. 2). The free Lys ε-$NH_2$ group is used for the coupling of the peptides to the SPR sensor surface in an unequivocal way. For SPR competition experiments the peptides were also prepared without a linker, in this case the carboxyl group of the connecting lysine was transformed to an amide.

### 3.2. SPR experiments of Grb2 binding to immobilized 1PP- and 2PP-surfaces

SPR binding experiments were performed with two types of SPR instruments. An IBIS II instrument with cuvette design easily allows long association times without consumption of large amounts of analyte in a flow. However, this instrument is less suitable to directly monitor rapid dissociation, as rebinding of analyte in the cuvette will strongly influence the dissociation phase. For simultaneous kinetic analysis of association and dissociation phase a Biacore 3000, applying a flow system, was used. Binding of Grb2 protein to SPR sensor surfaces with different degree of 2PP-immobilization, affecting the binding capacity, is shown in Fig. 3.

For the surface with the highest binding capacity (Fig. 3A), a steady increase is observed, before reaching equilibrium. For the medium and low capacity surfaces (Fig. 3B–F), the association phase as well as the dissociation phase is clearly biphasic. Upon injection of Grb2 protein an immediate rapid increase in signal occurs within a few seconds, followed by a much slower phase. The dissociation phase is also biphasic: rapid decay from the surface is followed by a much slower dissociation. The length of the association time and the binding capacity has an effect on the dissociation phase: the amount of slow dissociating species is clearly increased at longer association (compare Fig. 3C with Fig. 3E, and Fig. 3D with Fig. 3F).

Sensorgrams for the binding of Grb2 to 1PP-surfaces are shown in Fig. 4.

In the case of the 1PP-surface the association and dissociation also seem to be biphasic.

#### 3.2.1. Affinity of Grb2 derived from equilibrium SPR signals

The equilibrium SPR signal ($R_{eq}$) vs. [Grb2], for the high and medium capacity surfaces of 2PP could be fitted with a Langmuir binding isotherm (Eq. (1)), as shown in Fig. 5.

Despite the large differences in binding capacity, appearance of the kinetics (see Fig. 3), and instrumentation, the observed $K_{LM}$ values at equilibrium are consistent. In a similar way the $K_{LM}$ for binding of Grb2 to the Biacore 1PP-surface is assayed to be 3200 ± 400 nM (Fig. 5B).

From competition experiments the affinity of Grb2 in solution for **1PP** and **2PP** can be assayed [16]. Fig. 6 shows competition curves for Grb2 binding at equilibrium to a 2PP-surface in the presence of **1PP** and **2PP**. The affinity in solution ($K_S$) is 9800 ± 700 nM for **1PP**, and 630 ± 70 nM for **2PP**.

The affinity at equilibrium of **2PP** for Grb2 is similar at the surface, as well as in solution. For **1PP** there is a marked difference: 10 μM in solution and ~3 μM at a 1PP-surface. This can be explained by an avidity effect originating from one Grb2 molecule simultaneously binding to two **1PP** ligands on the surface (see Fig. 6B). The affinity of monovalent **1PP** of around 10 μM in solution agrees well with reported values of similar peptides for Grb2 C-SH3 and N-SH3 domains [8].

### 3.3. Kinetic analysis of SPR data

As the time-dependency of the SPR signal reflects the amount of bound material in real time, the underlying kinetics can be analyzed.

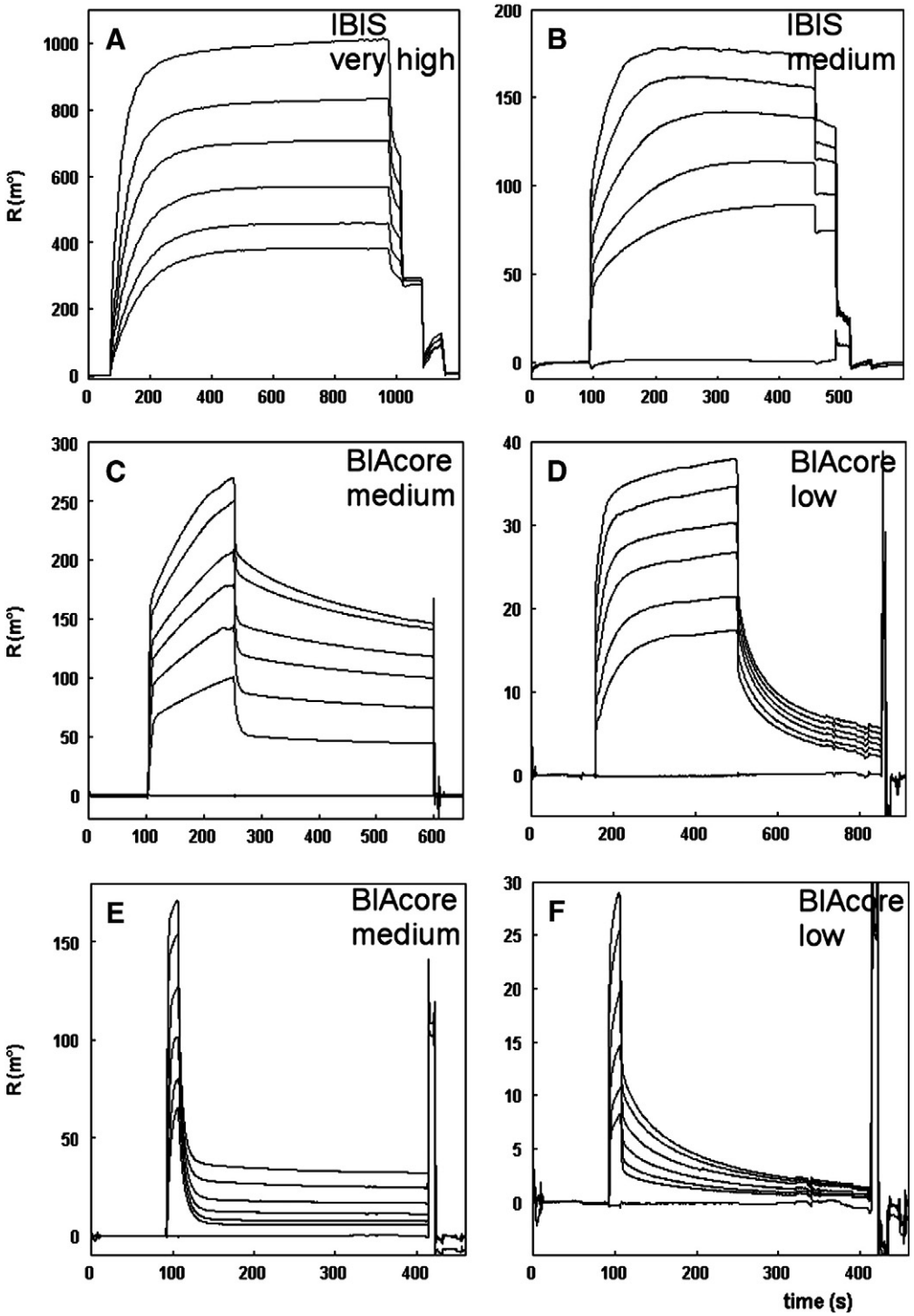


**Fig. 3.** Sensorgrams of binding of Grb2 protein to 2PP-SPR-surfaces as assayed with the IBIS II (panels A and B), and the Biacore 3000 (panels C–F). Surfaces with a very high (A), medium (B, C and E) and low binding capacity (D and F). Panels E and F are for the same surfaces as C and D, respectively, with short association time and high sampling rate (1 datapoint/0.4 s). Curves are for Grb2 added in a concentration range of 200 to 2000 nM.

The experimental sensorgrams can be fitted according to a predefined binding model. For this Morton and Myszka developed a computer program named CLAMP, which performs global fits of SPR curves [12]. This means that the same kinetic parameters, as defined by the binding model, are fitted to series of curves. In certain cases, especially with high binding capacity and/or high $k_{on}$ rates, the kinetics can be affected by mass transport limitation (MTL) [17,18]. MTL affects the association- as well as the dissociation phase to equal extent [18]. Under MTL conditions, in the association phase diffusion of analyte to the sensor surface becomes rate limiting, while in the dissociation phase rebinding occurs before the analyte diffuses away from the surface. Scheme 2 summarizes relevant binding models used in this study. In the binding models the transport step to account for MTL is represented by rate constant $k_{tr}$ for the diffusion of analyte from the bulk ($A_0$) to the sensor surface ($A$).

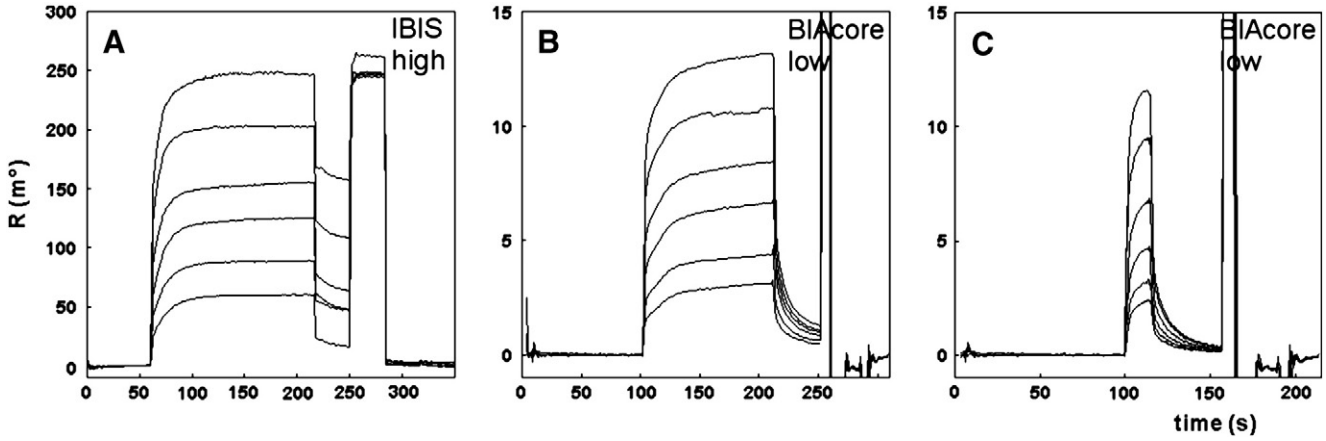


**Fig. 4.** Sensorgrams of Grb2 binding to 1PP-surfaces as assayed with IBIS II (panel A, high binding capacity surface) and Biacore 3000 (B and C, identical low binding capacity surface). Panel C: very short association time with high sampling rate (1 datapoint/0.4 s). Curves are for Grb2 in a range from 200 to 2000 nM.

In our data the association is so fast that it is generally necessary to include the transport rates in the models.

*3.3.1. Kinetic analysis of binding of Grb2 to 1PP-surfaces*

As shown in Fig. 4, the binding of Grb2 to immobilized **1PP** shows a biphasic course with extremely rapid initial association and dissociation, followed by slower association and dissociation. The binding at equilibrium to the 1PP-surface has a higher affinity than for **1PP** in solution. This indicates an avidity effect for Grb2 binding on the 1PP-surface. An obvious model for such binding is the AB–AB2 model (model 2, Scheme 2), in which the AB2 species occupies two **1PP** ligands on the surface (see Fig. 6B). Fits of the data for Grb2 binding to the 1PP-surface shown in Fig. 4, with the AB–AB2 model are presented in Fig. 7 for the IBIS data (only association) and Biacore data.

All these data can be described by the AB–AB2 model with bivalent binding to the 1PP-surface, despite the large difference in binding capacity of the surfaces. Fitting with a simple $A + B \leftrightarrows AB$ model including a transport step, gave much less satisfying results (results not shown). For the initial fast step in the AB–AB2 model ($A + B \leftrightarrows AB$) the kinetic parameters of the fits yield a $K_D$ value of around 10 μM. This value compares very well with that for monovalent binding of Grb2 to **1PP** in solution, which was estimated at 9.8 μM (Fig. 6). The results of these fits, together with the higher affinity of Grb2 for 1PP-surfaces compared to binding to **1PP** in solution (see above), strongly supports a major role of *inter*molecular bivalent binding of Grb2 to 1PP-surfaces (Fig. 6B).

*3.3.2. Kinetic analysis of Grb2 binding to 2PP-surfaces*

In a previous study we could analyze *intra*molecular bivalent binding with model **1** (see Scheme 2) [19]. The second step going from monovalent AB to bivalent AB* can be kinetically regarded as an *intra*molecular rearrangement. However, fits of data for Grb2 binding to 2PP-surfaces with this model were not satisfying (Fig. 8).

As an alternative for *intra*molecular bivalent binding, *inter*molecular bivalent binding was explored using the same AB-AB2 model as applied for the 1PP-surface. This model also gave no satisfying fits (see Supplementary data Fig. 3). However, formation of the AB2 species on a 2PP-surface in principle creates a site for capturing a second Grb2 molecule, with optimal distance between the two empty 2PP-epitopes

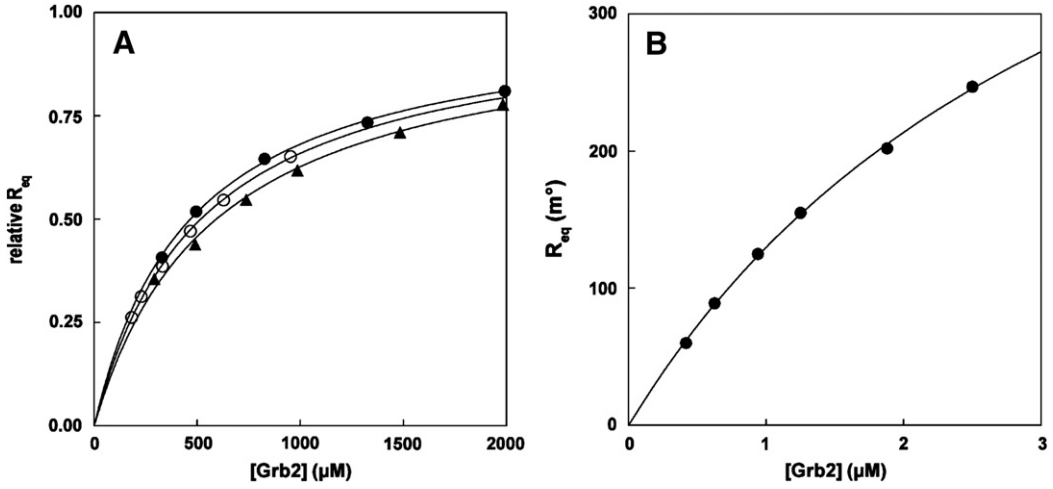


**Fig. 5.** Langmuir binding isotherms based on equilibrium SPR signals of Grb2 binding to 2PP (A) and 1PP (B) surfaces. Panel A: the IBIS high capacity (data Fig. 3A, open circles) and medium capacity 2PP-surfaces (data Fig 3B, closed circles). Also included are the data from the equilibrium signal of the Biacore low capacity 2PP-surface (data Fig. 3D, closed triangles). For clarity the SPR signals have been normalized to a maximum binding capacity of 1. Derived $K_{LM}$-values from fits with Eq. (1) (Materials and methods): $520 \pm 20$ and $470 \pm 20$ nM for high and medium capacity IBIS surfaces, respectively. $K_{LM}$ for the Biacore surface is $585 \pm 50$ nM. Panel B: binding to a 1PPsurface (data Fig. 4A). Derived $K_{LM}$-value $3.2 \pm 0.4$ μM.

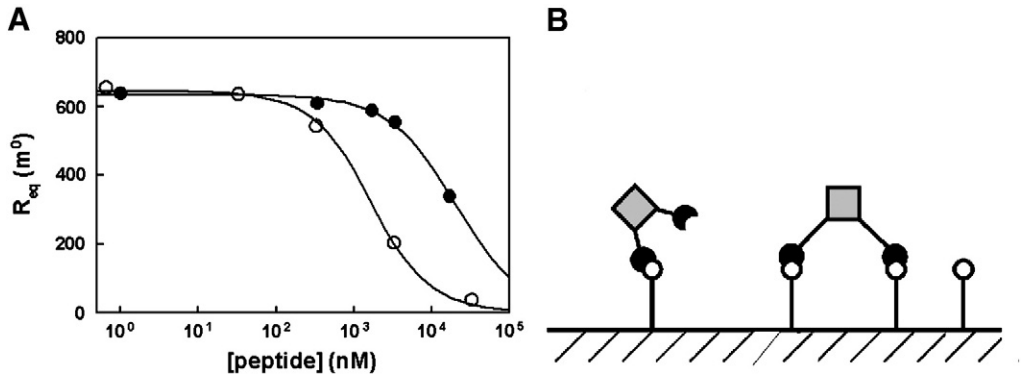


**Fig. 6.** A: SPR competition experiment with 500 nM Grb2 binding to a 2PP-surface in the presence of **1PP** (closed circles) and **2PP** (open circles). The lines are the fits according to the model previously described [16]. Values for the $K_D$ in solution ($K_S$) are 9800 ± 700 nM for **1PP** and 630 ± 70 nM for **2PP**. B: bivalent binding of Grb2 to a 1PP-surface.

(Scheme 1B). The AB-AB2-A2B2 model (Scheme 2, model 3) takes the necessary steps into account. Fits with model 3 of data for Grb2 binding to 2PP-surfaces (see Fig. 3), are shown in Fig. 9.

The association phases obtained from the IBIS instrument for various binding capacity surfaces could be fitted very well with the AB-AB2-A2B2 model. The data from the Biacore instrument also includes the dissociation phase. For the medium high binding capacity and longer association (9C) excellent fits are obtained for the three lowest concentrations, however deviations occur at higher Grb2 concentrations (>1 μM). Possibly, the higher SPR signal than predicted by the model, is caused by the formation of cross-links in the SPR sensor matrix due to bivalent binding, which may make the sensor matrix more compact and closer to the gold surface, resulting in a higher intrinsic SPR signal [20]. This effect is expected to be larger for lower capacity surfaces, as the distance to a second binding partner is increased. Indeed, the lower capacity surface is again well fitted for only the three lowest concentrations (Fig. 9D). With short association the data for the medium and low capacity surface can be well described by model 3 for all concentrations (Fig. 9E and F). At short association time less cross-linking of the sensor matrix will occur. The superiority of model 3 is illustrated in Fig. 3 (Supplementary data). The RSSq values for fits with model 1, 2 and 3 is 5.0, 6.5 and 1.1, respectively.

| **1**. *Intra*molecular bivalent binding model | **2**. Divalent *inter*molecular model | **3**. *inter*molecular bivalent dimer model |
|---|---|---|
| $A_0 \underset{k_{-tr}}{\overset{k_{tr}}{\Leftrightarrow}} A$<br>$A + B \underset{k_{off}}{\overset{k_{on}}{\Leftrightarrow}} AB$<br>$AB \underset{k_{-conf}}{\overset{k_{conf}}{\Leftrightarrow}} AB^*$ | $A_0 \underset{k_{-tr}}{\overset{k_{tr}}{\Leftrightarrow}} A$<br>$A + B \underset{k_{off}}{\overset{k_{on}}{\Leftrightarrow}} AB$<br>$AB + B \Leftrightarrow AB2$ | $A + B \underset{k_{off}}{\overset{k_{on}}{\Leftrightarrow}} AB$<br>$AB + B \underset{k_{rev}}{\overset{k_{biv}}{\Leftrightarrow}} AB2$<br>$AB2 + A \underset{k_{off}}{\overset{k_{on}}{\Leftrightarrow}} A2B2$ |

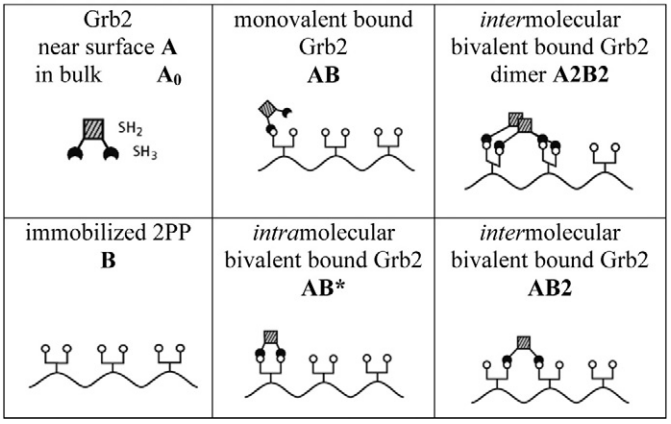


**Scheme 2.** Kinetic models for binding to the bivalent 2PP-surface applied in this study (upper panel), and species defined in these models (lower panel).

### *3.4. Evaluating Grb2 dimer formation in solution by chemical cross-linking and dynamic light scattering*

The kinetic analysis of Grb2 binding to 2PP-surfaces strongly supports major contributions of the bivalent *inter*molecular binding model 3 (Scheme 2). An intriguing feature of this model is the possible formation of Grb2 dimers in the A2B2 species. In the X-ray structure of Grb2 an embedded Grb2 dimer in the asymmetric unit is found with a quite large dimer interface [21]. However, the different reports on the occurrence of a monomer/dimer equilibrium appeared: Grb2 dimers in diluted solutions could not be demonstrated [21]. Evidence for a (weak) monomer/dimer equilibrium with a $K_{dim}$ of ~30 μM is reported by McDonald et al. [22]. Schiering et al. reported another type of dimer upon expression of the Grb2 SH2 domain as a GST fusion protein: a domain swapped dimer which is in a metastable state [23]. We observed that stable full-length Grb2 dimers are formed, which are not in equilibrium with the monomer, and can be isolated in pure form (see Materials and methods). Apparently our dimer deviates from that reported by McDonald et al. [22]. The possible formation of Grb2 dimers in the presence of **2PP** prompted us to study this with two independent assays: chemical cross-linking and dynamic light scattering (DLS).

Chemical cross-linking experiments were performed with 10 μM Grb2 in the presence or absence of 0.2 mM **2PP**. Based on the $K_{LM}$-value, under these conditions >99% of the Grb2 is in complex with **2PP**. Cross-linking reagent glutaraldehyde was used in concentrations of 0.01, 0.1 and 1%. Grb2 dimer, which was isolated and purified during the GST fusion protein expression procedure (see Materials and methods), was used as a positive control. Applying 0.01% glutaraldehyde, this preformed Grb2 dimer was almost completely cross-linked (Fig. 10A). For Grb2 monomer, whether or not in the presence of **2PP**, such cross-linked dimers are not observed with any glutaraldehyde concentration.

With DLS experiments the effect of **2PP** on the particle size distribution of a Grb2 solution was studied. For a 0.8 μM Grb2 solution without **2PP**, a sharp peak is observed (Fig. 10B), which is representative for a globular particle with a diameter of 5.5 nm. Grb2 has an extended flexible structure with a maximum dimension value of 8 nm [9]. Therefore, a value of 5.5 nm corresponds well to what is expected for a Grb2 monomer. Upon addition of 0.2 mM **2PP** the sharp peak of the Grb2 monomer remains identical.

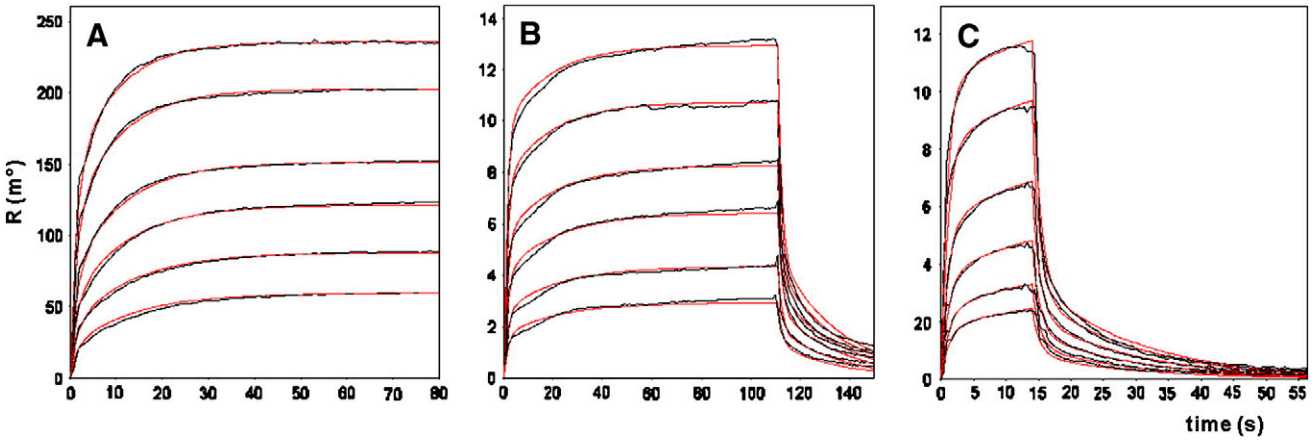


**Fig. 7.** Kinetic analysis of Grb2 binding to 1PP-surfaces with the AB–AB2 model. A: a high binding capacity 1PP-surface assayed with the IBISII. B and C: a low binding capacity surface assayed with the Biacore, with long (B) and short (C) association.

These experiments yield no indications that **2PP** induces the formation of A2B2 species in solution. Additionally, from ESI-MS spectra under mild conditions, of Grb2 and Grb2-2PP complexes, no indications for dimerization can be derived neither (Dr. Isabel Catalina, personal communication). These results indicate that the dimeric interface of Grb2, as observed in the X-ray structure, is not involved in the formation of complexes of 2PP with Grb2 in solution.

### *3.5. Effect of association time on displacement of Grb2 from 2PP-surfaces by 1PP*

Intermolecular binding is an essential step in binding model 3, leading to the A2B2 species on the 2PP-surface (Scheme 2). It is expected for such binding model that the association time is relevant for the contribution of weak (e.g. AB) and tighter binding species (e.g. A2B2). To study this, the effect of the association time on displacement of Grb2 from the surface by addition of **1PP** was studied at two time intervals: short after exposure of Grb2 to the surface, and upon reaching binding equilibrium (Fig. 11).

Association on a 2PP-surface during 10 s, results in larger displacement than at equilibrium. Similar results have also been obtained performing the experiment on a 1PP-surface (results not shown). This supports the conclusion that the initial fast association and dissociation phases (see Figs. 7 and 9) can be attributed to formation of weaker binding species (AB), and the slower association and dissociation to stronger binding species (AB2, A2B2).

### *3.6. Modeling of the A2B2 species*

The above described experiments are consistent with a binding mode with major contribution of *inter*molecular bivalent binding and docking of a second Grb2 molecule at the 2PP-surface, ultimately leading to the A2B2 species. To further explore the possibility that an A2B2 species can be formed, a 3D model of A2B2, allowing *inter*molecular **2PP** binding, was generated. This A2B2 model is based on the X-ray Grb2 dimer structure in a modeled complex with two *intra*molecular bivalent binding 2PP-peptides (see Figs. 1B and 12A). To obtain a model for *inter*molecular bivalent binding of **2PP** (A2B2), the N-SH3 domain of Grb2 molecule 1 is swapped with the N-SH3 domain of molecule 2 (see Fig. 12A). In this swapped model the SH3 domains are at the same distance and orientation for bivalent binding of **2PP** in the class II mode, as in the *intra*molecular model (Fig. 1B). The linker length between N-SH3 and SH2 domain appears to be long enough to allow such swap.

In this model the dimer interface between the Grb2 molecules remains completely intact, as the N-SH3 domains are not involved in dimer contacts. Now the Grb2 is no longer in a closed conformation as shown in Fig. 1B, but the N-SH3 domain has flipped to a more open conformation (Fig. 12B).

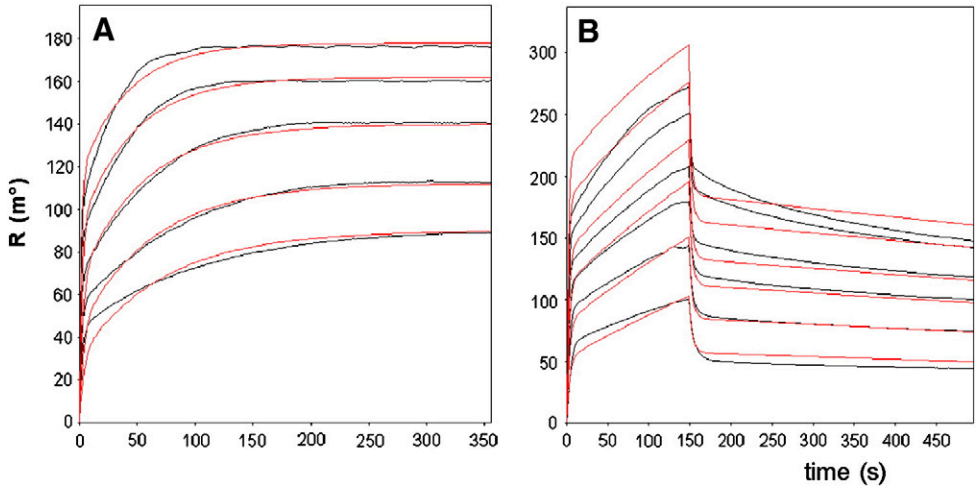


**Fig. 8.** Kinetic analysis of Grb2 binding to 2PP-surfaces with the *intra*molecular bivalent model (AB–AB* model, Scheme 2, model 1). Panel A data from IBIS platform (data Fig. 3B). Panel B data from Biacore platform (data Fig. 3C).

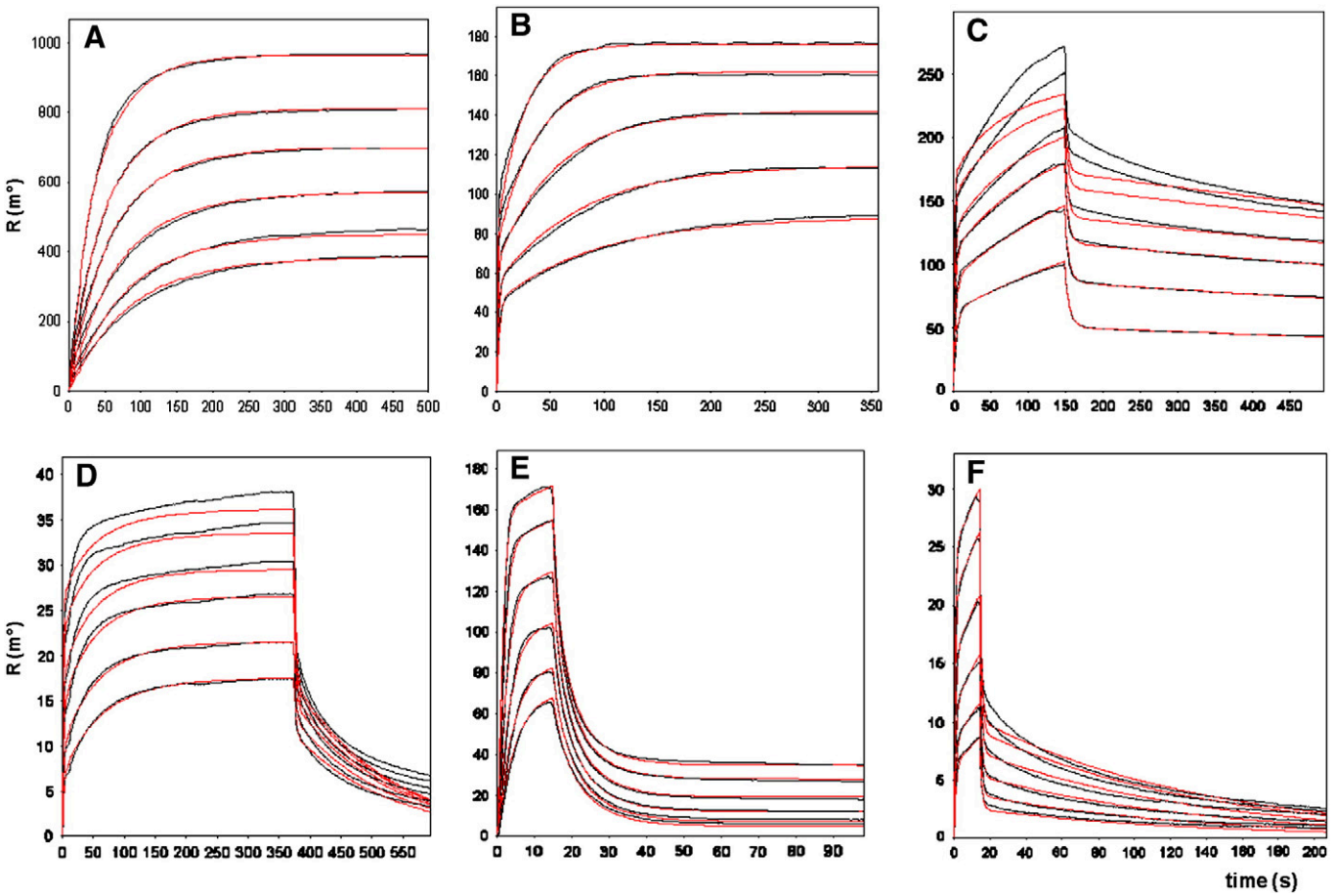


**Fig. 9.** Kinetic analysis of Grb2 binding to 2PP-surfaces with the AB–AB2–A2B2 model (Scheme 2, model **3**). Panels A and B: data from the IBIS instrument with high (A) and medium binding capacity (B). C–F data from Biacore for medium (C and E) and low binding capacity (D and F), with longer (C and D), and short association (E and F). Grb2 concentrations are from 0.2 to 2 μM. For C and D only the lowest three concentrations were fitted (see Section 3.3.2.).

## 4. Discussion

The kinetic behavior of Grb2 binding to a bivalent 2PP-surface is quite deviant from what we have observed for other bivalent systems, e.g. the binding of Syk tandem SH2 to ITAM derived ligands [24]. In the latter case the kinetics could be explained by monovalent binding, which is followed by *intra*molecular bivalent binding (Scheme 2, model 1 AB* species). This model appeared not to be satisfying for the binding of Grb2 to 2PP (Fig. 8 and Supplementary data Fig. 3A). The affinity of Grb2 to the 2PP surface is definitely higher than monovalent **1PP** binding, suggesting involvement of a deviant type of bivalent binding. The kinetic analysis of Grb2 binding to 1PP- and 2PP-surfaces is in accordance with major contributions from *inter*molecular bivalent binding as described by model 2. For the 2PP-surface this yields a docking site for a second Grb2 molecule (Scheme 1). Without inclusion of binding of this second Grb2 in the kinetic model the data are poorly described. In the kinetic modeling of Grb2 binding to the 2PP-surface this second Grb2 binding has to

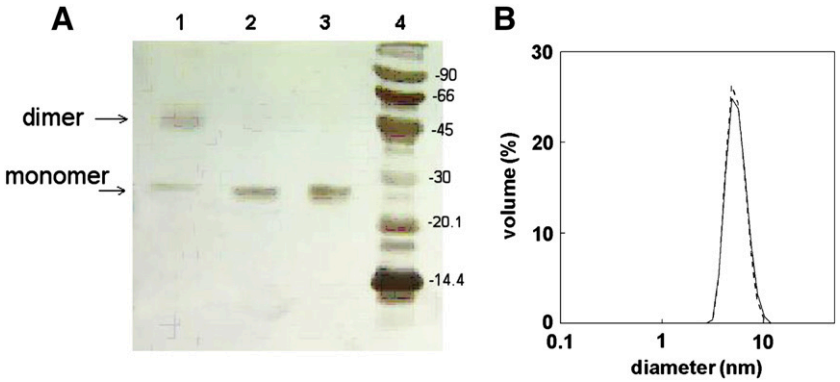


**Fig. 10.** (A) SDS PhastGel® of chemical cross-linking experiments with Grb2 (10 μM) with 0.01% glutaraldehyde. Lane 1: preformed Grb2 dimer, lane 2 Grb2 (monomer) in the presence of 0.2 mM **2PP**, lane 3 Grb2 without **2PP**, lane 4: molecular weight markers. (B) Particle size distribution by volume as assayed by dynamic light scattering (DLS). $8\times10^{-5}$ M Grb2 without **2PP** (solid line) or with $2\times10^{-4}$ M **2PP** (dotted line).

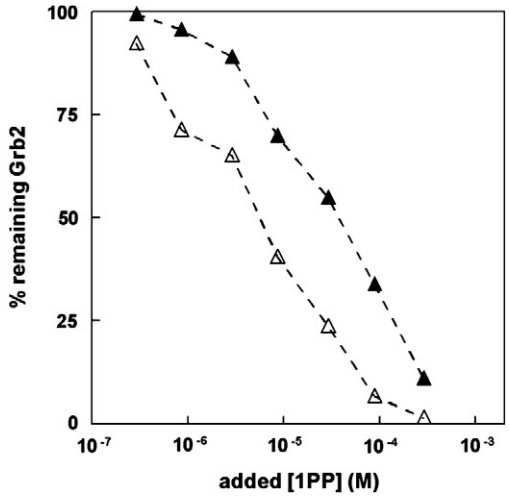


**Fig. 11.** Displacement of Grb2 from a 2PP-SPR surface by **1PP** in various concentrations. Grb2 (1 μM) was injected to a 2PP-SPR sensor surface. **1PP** was added after 10 s (open triangles) or after reaching equilibrium (closed triangles).

be included (model 3) to obtain good fits (see Fig. 9 and Supplementary data Fig. 3B).

To the best of our knowledge such *inter*molecular double binding model for bivalent binding has not been presented before. The question arises why does it occur? Apparently, here *inter*molecular binding at the surface is preferred over *intra*molecular. An obvious explanation would be that the distance between the polyproline epitopes in **2PP** is not optimal for *intra*molecular binding to Grb2. However, considerably increasing the linker length in similar peptides as **2PP** with one or two aminohexanoic spacers has no effect on the affinity of bivalent PP ligands [25]. Only when a very short diamino propanoic acid spacer is used, instead of lysine like in **2PP**, bivalent binding is lost [25]. Therefore a short inter-PP distance is not a likely explanation.

The thermodynamics of (*intra*molecular) bivalent systems has been evaluated by Whitesides et al. [26]. Monovalent binding is preferred, if the entropy for monovalent binding (mainly rotational and translational entropy) is more favorable than the conformational entropy involved in the second step in *intra*molecular bivalent binding [26]. It is possible that this situation also applies here to hamper *intra*molecular bivalent binding to the surface. Studies of the structure of Grb2 in solution show that the SH3 domains are connected to the SH2 domain with flexible linkers. The inter-SH3 distance distribution derived from molecular dynamics indicates a broad range of distances with a peak at 50 Å and a half width of 40 Å [9]. This flexibility may yield more profitable entropy in *inter*molecular binding, where the distance between the two SH3-binding epitopes is not so rigid as in *intra*molecular bivalent binding. In the *intra*molecular complex with **2PP**, Grb2 is forced in a closed conformation (see Fig. 1B), with little degrees of freedom for the SH2–SH3 linkers. The swapped A2B2 structural model, based on the X-ray Grb2-dimer, shown in Fig. 12 shows that the flexible SH2–SH3 linkers can adapt to a more open conformation. Inspection of the model suggests that the SH2–SH3 linkers in the A2B2 model have more degrees of freedom than in the *intra*molecular binding mode.

Another condition favoring *inter*molecular binding is the high local concentration of binding sites within the dextran layer on the SPR sensor surface, which makes it easier to find a second 2PP-epitope. Taking into account that 1 m° of SPR signal corresponds to 10 pg/mm$^2$, the local concentration of Grb2 in the 100 nm sensor matrix layer for 1 m° is estimated to be 4 μM. For a medium high capacity surface of 200 m°, the local concentration of 2PP-epitopes will be as high as 0.8 mM. Bivalent binding at a surface is different from bivalent binding in solution. After monovalent binding of bivalent Grb2 at the surface, the second binding site must be within reach of the still unbound SH3-domain, although it must be kept in mind that the dextran matrix of the SPR sensor has some flexibility. A high local concentration of PP-sequences on the SPR surface will favor *inter*molecular bivalent binding.

The X-ray structure of Grb2 shows a substantial dimer interface [21]. This may favor the formation of the A2B2 species, where two Grb2 molecules are forced close to each other. The swapped model

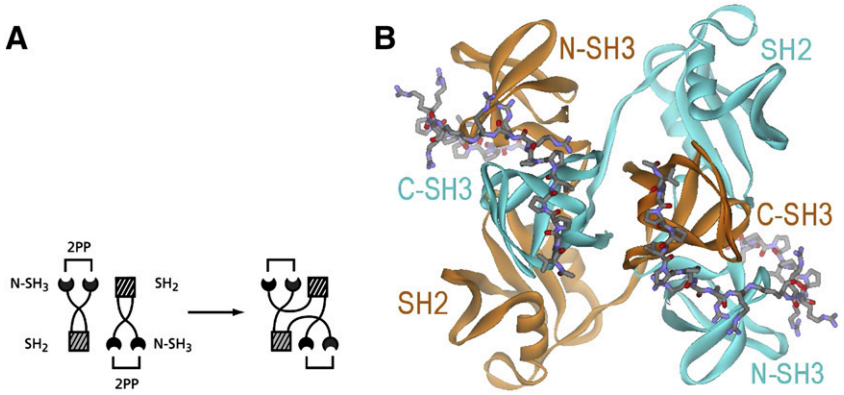


**Fig. 12.** A2B2 model for bivalent *inter*molecular binding. (A) The model is derived from the X-ray dimer structure by swapping of the N-SH3 domains. (B): the A2B2 model showing the swapped N-SH3 domains, with Grb2 in a more open conformation. The Grb2-dimer interface remains as in the X-ray dimer. The two *inter*molecularly bound **2PP** ligands are shown as sticks.

shown in Fig. 12, demonstrates that an A2B2 species is possible with conservation of the extended dimer interface observed in the X-ray structure. The existence of weak dynamic Grb2 monomer/dimer equilibrium is reported [22]. Additional interactions at the dimer interface should certainly favor the A2B2 binding model. We have not observed such equilibrium for our Grb2. Part of the protein is expressed as a stable dimer, that could be isolated. Furthermore, we could not demonstrate Grb2 dimer formation upon binding to **2PP** in solution (Fig. 11). However, this does not rule out a role for Grb2 dimerization at the high local concentration on our SPR surfaces.

The affinity of Grb2 binding to **2PP** in solution and to 2PP-surfaces is comparable. In both processes the major contributions to the binding energy from SH3–PP interactions will be similar, including the avidity effect. Apparently, the total sum of other contributions related to surface or solution, like rotational, conformational and translational entropy, is not very different. We assume that in solution *intra*molecular binding is preferred (no indications for dimers). The comparable binding energy for *intra*- and *inter*molecular binding makes them competitive processes, and both binding modes may occur simultaneously at the surface in various ratios.

We think that the *inter*molecular binding mode might also occur in a cellular environment. The similar affinity compared to *intra*molecular binding suggests that it could be competitive with *inter*molecular binding, provided a high local concentration of *inter*molecular binding sites is present in aggregated protein complexes. The C-terminus of Sos proteins has a high density of PP-sequences. When enough Grb2 molecules are available this could lead to crowding and steric hindrance upon *intra*molecular binding. In such situation *inter*molecular binding with one Grb2 molecules interacting with two proline-rich proteins will be favorable. Also Grb2 dimers might be involved in *inter*molecular binding. Recent work indicates that dimeric Grb2 plays a role in the control of FGF-receptor regulation, and formation of the Grb2–Gab1 complex [27,28].

SH3 domains are abundant in aggregation of large multiprotein complexes [10]. The affinity of one SH3 domain with one PP sequence is rather low at 10 μM. The SH3 function is to bring proteins together. To explain the selectivity of these low affinity domains in protein aggregation Mayer proposes that SH3 domains are involved in non-linear multiprotein networks [10]. Not every protein binds to one other protein, but a protein simultaneously interacts with more proteins in a variety of dynamic complexes. In such multi-protein complexes intermolecular multivalent binding is crucial. The results of this study, with one Grb2 molecule binding to two different 2PP-epitopes fit well in this concept.

## 5. Conclusion

The bivalent binding of Grb2 to a proline-rich bivalent surface shows unusual kinetics that can be explained by the major contribution of a binding model that proceeds via monovalent- and *inter*molecular bivalent binding, resulting in binding of a second Grb2 molecule (A2B2 complex). This binding mode was quite unexpected and has not been reported before as an alternative for bivalent binding on a surface. Two conditions might explain this deviant behavior. Firstly, more favorable entropy for the flexible Grb2 in *inter*molecular complexes AB2 and A2B2, compared to the *intra*molecular complex AB* (Scheme 2), with Grb2 in a closed more rigid conformation. Secondly, the high local concentration of 2PP-epitopes on the SPR surface will also enhance *inter*molecular binding.

Grb2 interacts with the Sos protein, which contains at least seven different proline-rich consensus sequences in the C-terminus, for binding to SH3 domains in either class I or class II mode. Next to this, several other sequences are present that might also bind to Grb2 SH3 domains [29]. A high density of SH3 ligands on aggregating protein complexes might contribute to participation of *inter*molecular binding in a cellular environment. The importance of *inter*molecular SH3-mediated interactions of multiple SH3 domains containing proteins in dynamic multi-protein complexes has been emphasized by Mayer [10]. Such *inter*molecular interactions of Grb2 excellently fit in a non-linear complex dynamic network of protein aggregation with multiple mutual interactions of each component.

The results of this study are also relevant for design of ligands that interfere in Grb2-mediated interactions. Constructs with multiple SH3 ligands close together, are expected to be very potent. Such constructs could be realized by attaching multiple SH3-ligands on a scaffold or by functionalizing dendrimers with SH3-ligands.


## Acknowledgements

We thank Prof. Jurriaan Huskens (Twente University) for stimulating discussions on binding models for 2D “printboard” surfaces compared to SPR sensor surfaces, and Mr Mies van Steenbergen (Utrecht University) for help in the DLS measurements. We thank Dr Marcel Fischer (Utrecht University) for support in the protein cross-linking experiments.


## Appendix A. Supplementary data

Supplementary data to this article can be found online at http://dx.doi.org/10.1016/j.bbapap.2012.11.001.

## References


[1] A. Yart, P. Mayeux, P. Raynal, Gab1, SHP-2 and other novel regulators of Ras: targets for anticancer drug discovery? Curr. Cancer Drug Targets 3 (2003) 177–192.
[2] J.A. Simon, S.L. Schreiber, Grb2 SH3 binding to peptides from Sos: evaluation of a general model for SH3-ligand interactions, Chem. Biol. 2 (1995) 53–60.
[3] C.B. McDonald, K.L. Seldeen, B.J. Deegan, A. Farooq, SH3 domains of Grb2 adaptor bind to PXψPXR motifs within the Sos1 nucleotide exchange factor in a discriminate manner, Biochemistry (N. Y.) 48 (2009) 4074–4085.
[4] C.B. McDonald, K.L. Seldeen, B.J. Deegan, V. Bhat, A. Farooq, Assembly of the Sos1-Grb2-Gab1 ternary signaling complex is under allosteric control, Arch. Biochem. Biophys. 494 (2010) 216–225.
[5] B. Gay, S. Suarez, G. Caravatti, P. Furet, T. Meyer, J. Schoepfer, Selective Grb2 SH2 inhibitors as anti-Ras therapy, Int. J. Cancer 83 (1999) 235–241.
[6] S.M. Feller, G. Tuchscherer, J. Voss, High affinity molecules disrupting GRB2 protein complexes as a therapeutic strategy for chronic myelogenous leukaemia, Leuk. Lymphoma 44 (2003) 411–427.
[7] P.G. Dharmawardana, B. Peruzzi, A. Giubellino, T.R. Burke Jr., D.P. Bottaro, Molecular targeting of growth factor receptor-bound 2 (Grb2) as an anti-cancer strategy, Anticancer Drugs 17 (2006) 13–20.
[8] D. Cussac, M. Vidal, C. Leprince, W. Liu, F. Cornille, G. Tiraboschi, B.P. Roques, C. Garbay, A Sos-derived peptidimer blocks the Ras signaling pathway by binding both Grb2 SH3 domains and displays antiproliferative activity, FASEB J. 13 (1999) 31–38.
[9] S. Yuzawa, M. Yokochi, H. Hatanaka, K. Ogura, M. Kataoka, K. Miura, V. Mandiyan, J. Schlessinger, F. Inagaki, Solution structure of Grb2 reveals extensive flexibility necessary for target recognition, J. Mol. Biol. 306 (2001) 527–537.
[10] B.J. Mayer, SH3 domains: complexity in moderation, J. Cell Sci. 114 (2001) 1253–1263.
[11] J.P. Guilloteau, N. Fromage, M. Ries-Kautt, S. Reboul, D. Bocquet, H. Dubois, D. Faucher, C. Colonna, A. Ducruix, J. Becquart, Purification, stabilization, and crystallization of a modular protein: Grb2, Proteins Struct. Funct. Genet. 25 (1996) 112–119.
[12] T.A. Morton, D.G. Myszka, Kinetic analysis of macromolecular interactions using surface plasmon resonance biosensors, Methods Enzymol. 295 (1998) 268–294.
[13] G. Vriend, C. Sander, Detection of common three-dimensional substructures in proteins, Proteins Struct. Funct. Genet. 11 (1991) 52–58.
[14] E. Krieger, T. Darden, S.B. Nabuurs, A. Finkelstein, G. Vriend, Making optimal use of empirical energy functions: force-field parameterization in crystal space, Proteins Struct. Funct. Genet. 57 (2004) 678–683.
[15] J. Wang, P. Cieplak, P.A. Kollman, How well does a Restrained Electrostatic Potential (RESP) model perform in calculating conformational energies of organic and biological molecules? J. Comput. Chem. 21 (2000) 1049–1074.
[16] N.J. de Mol, M.B. Gillies, M.J.E. Fischer, Experimental and calculated shift in pKa upon binding of phosphotyrosine peptide to the SH2 domain of p56lck, Bioorg. Med. Chem. 10 (2002) 1477–1482.
[17] N.J. de Mol, M.J. Fischer, Surface plasmon resonance: a general introduction, Methods Mol. Biol. 627 (2010) 1–14.
[18] P. Schuck, H. Zhao, The role of mass transport limitation and surface heterogeneity in the biophysical characterization of macromolecular binding processes by SPR biosensing, Methods Mol. Biol. 627 (2010) 15–54.
[19] N.J. De Mol, M.I. Catalina, F.J. Dekker, M.J.E. Fischer, A.J.R. Heck, R.M.J. Liskamp, Protein flexibility and ligand rigidity: a thermodynamic and kinetic study of

ITAM-based ligand binding to Syk tandem SH2, Chembiochem 6 (2005) 2261–2270.
[20] E.T. Gedig, Surface chemistry in SPR technology, in: R.B.M. Schasfoort, A.J. Tudos (Eds.), Handbook of Surface Plasmon Resonance, RSC Publishing, Cambridge, UK, 2008, p. 173.
[21] S. Maignan, J. Guilloteau, N. Fromage, B. Arnoux, J. Becquart, A. Ducruix, Crystal structure of the mammalian Grb2 adaptor, Science 268 (1995) 291–293.
[22] C.B. McDonald, K.L. Seldeen, B.J. Deegan, M.S. Lewis, A. Farooq, Grb2 adaptor undergoes conformational change upon dimerization, Arch. Biochem. Biophys. 475 (2008) 25–35.
[23] N. Schiering, E. Casale, P. Caccia, P. Giordano, C. Battistini, Dimer formation through domain swapping in the crystal structure of the Grb2-SH2-Ac-pYVNV complex, Biochemistry (N. Y.) 39 (2000) 13376–13382.
[24] N.J. De Mol, M.I. Catalina, F.J. Dekker, M.J.E. Fischer, A.J.R. Heck, R.M.J. Liskamp, Protein flexibility and ligand rigidity: a thermodynamic and kinetic study of ITAM-based ligand binding to Syk tandem SH2, Chembiochem 6 (2005) 2261–2270.
[25] M. Vidal, W. Liu, C. Lenoir, J. Salzmann, N. Gresh, C. Garbay, Design of peptoid analogue dimers and measure of their affinity for Grb2 SH3 domains, Biochemistry (N. Y.) 43 (2004) 7336–7344.
[26] M. Mammen, S. Choi, G.M. Whitesides, Polyvalent interactions in biological systems: implications for design and use of multivalent ligands and inhibitors, Angew. Chem. Int. Ed. 37 (1998) 2755–2794.
[27] C. Lin, F.A. Melo, R. Ghosh, K.M. Suen, L.J. Stagg, J. Kirkpatrick, S.T. Arold, Z. Ahmed, J.E. Ladbury, Inhibition of basal FGF receptor signaling by dimeric Grb2, Cell 149 (2012) 1514–1524.
[28] C.B. McDonald, V. Bhat, D.C. Mikles, B.J. Deegan, K.L. Seldeen, A. Farooq, Bivalent binding drives the formation of the Grb2–Gab1 signaling complex in a noncooperative manner, FEBS J. 279 (2012) 2156–2173.
[29] N. Zarich, J.L. Oliva, R. Jorge, E. Santos, J.M. Rojas, The isoform-specific stretch of hSos1 defines a new Grb2-binding domain, Oncogene 19 (2000) 5872–5883.